Evaluation of Isoprene Nitrate Chemistry in Detailed Chemical Mechanisms

Alfred W. Mayhew[1], Ben H. Lee[2], Joel A. Thornton[2], Thomas J. Bannan[3], James Brean,[4] James R. Hopkins[1,5], James D. Lee[1,5], Beth S. Nelson[1], Carl Percival[3], Andrew R. Rickard[1,5], Marvin D. Shaw[1,5], Peter M. Edwards[1], Jaqueline F. Hamilton[1]

[1]Wolfson Atmospheric Chemistry Laboratories, Department of Chemistry, University of York, Heslington, York, UK
[2]Department of Atmospheric Sciences, University of Washington Seattle, Washington 98195, USA
[3]School of Earth and Environmental Sciences, University of Manchester, Manchester, UK
[4]School of Geography, Earth and Environmental Sciences, University of Birmingham, Birmingham, U.K.
[5]National Centre for Atmospheric Science, University of York, York, UK

Correspondence to: Jaqueline F. Hamilton (jacqui.hamilton@york.ac.uk)

Abstract. Isoprene nitrates are important chemical species in the atmosphere which contribute to the chemical cycles that form ozone and secondary organic aerosol (SOA) with implications for climate and air quality. Accurate chemical mechanisms are important for the prediction of the atmospheric chemistry of species such as isoprene nitrates in chemical models. In recent years, studies into the chemistry of isoprene nitrates have resulted in the development of a range of mechanisms available for use in the simulation of atmospheric isoprene oxidation. This work uses a 0-D chemical box-model to assess the ability of three chemically detailed mechanisms to predict the observed diurnal profiles of four groups of isoprene-derived nitrates in the summertime in the Chinese Megacity of Beijing. An analysis of modelled $C_5H_9NO_5$ isomers, including isoprene hydroperoxy nitrate (IPN) species, highlights the significant contribution of non-IPN species to the $C_5H_9NO_5$ measurement, including the potentially large contribution of nitrooxy hydroxyepoxide (INHE). The changing isomer distribution of isoprene hydroxy nitrates (IHN) derived from OH-initiated and NO3-initiated chemistry is discussed, as is the importance of up-to-date alkoxy radical chemistry for the accurate prediction of isoprene carbonyl nitrate (ICN) formation. All mechanisms reasonably reproduced $C_4H_7NO_5$ as predominately formed from the major isoprene oxidation products, methyl vinyl ketone (MVK) and methacrolein (MACR). This work explores the current capability of existing chemical mechanisms to accurately represent isoprene nitrate chemistry in urban areas significantly impacted by anthropogenic and biogenic chemical interactions, suggests considerations to be taken when applying these mechanisms to ambient scenarios, and makes some proposals for the future development of isoprene mechanisms.

1 Introduction

Isoprene (2-methyl-1,3-butadiene) is the most emitted non-methane volatile organic compound (NMVOC) globally, and accounts for around 70% of global biogenic volatile organic compound (BVOC) emissions.(Guenther et al., 1995; Guenther et al., 2006; Guenther et al., 2012; Sindelarova et al., 2014) Isoprene is a dialkene, and so is susceptible to oxidation in the

atmosphere, initiated by the breaking of one, or both, of the double bonds.(Wennberg et al., 2018) Some of the products of these reactions are organonitrates which are formed either by the reaction of isoprene with hydroxyl radicals (OH) and

35   subsequent reactions with O_2 and NO, or by the addition of the nitrate radical (NO_3) to one of isoprene's double bonds. The resulting nitrates are important for their influence on the NO_x, HO_x, and O_3 budgets, as well as the potential for the formation of secondary organic aerosol (SOA) by condensation or via further reactions.(Emmerson and Evans, 2009; Bates and Jacob, 2019; Schwantes et al., 2019; Schwantes et al., 2020; Vasquez et al., 2020; Palmer et al., 2022)

This work focusses on three types of primary nitrates resulting from isoprene oxidation, and one group of secondary nitrates.

40   The primary C_5 nitrates are the isoprene hydroxynitrates (IHN, Figure 1), isoprene carbonyl nitrates (ICN, Figure 2), and isoprene hydroperoxynitrates (IPN, Figure 3). The molecular formulae of IHN, ICN, and IPN are $C_5H_9NO_4$, $C_5H_7NO_4$, and $C_5H_9NO_5$, respectively. Throughout this work an upper-case sigma is used to denote the group of nitrates as well as any other species present in a chemical mechanism with the same molecular formula. For example, ΣIHN will refer to all isoprene hydroxynitrates as well as any other $C_5H_9NO_4$ species present in each chemical mechanism. A glossary of the terms

45   used to refer to different nitrated species is given in the supplementary information (Table S4).

IHN may be formed by OH-initiated oxidation followed by a peroxy radical (RO_2) + NO reaction, or by NO_3-initiated oxidation followed by RO_2 cross-reactions to form the alcohol group (Figure 1). ICN is formed by NO_3-initiated oxidation followed by RO_2 cross-reactions, hydrogen abstraction from alkoxy radicals (RO) by oxygen (RO + O_2 → ICN + HO_2), or the reaction of IPN or isoprene dinitrates (IDN) with OH (Figure 2). IPN is formed by NO_3-initiated oxidation followed by

50   RO_2 + HO_2 reactions (Figure 3).(Jenkin et al., 2015; Wennberg et al., 2018; Novelli et al., 2021; Vereecken et al., 2021)

The final group of nitrates are secondary nitrates with the formula $C_4H_7NO_5$, corresponding to the hydroxycarbonyl nitrate structures shown in Figure 4, which have been shown to be a major contributor to isoprene nitrates as measured by iodide chemical ionisation mass spectrometry (I^--CIMS).(Tsiligiannis et al., 2022 (under review)) $ΣC_4H_7NO_5$ refers to the isoprene-derived nitrates as well as isomeric species present in the Master Chemical Mechanism (MCM) from other VOC

55   sources.(Jenkin et al., 2015) There are several identified formation routes of $C_4H_7NO_5$ including the OH-initiated oxidation of methyl vinyl ketone (MVK) and methacrolein (MACR); NO_3-initiated oxidation of MVK and MACR; OH-initiated oxidation of IHN, IPN, and ICN; the ozonolysis of IHN; and the NO_3-initiated oxidation of hydroxycarbonyls (Figure 5).(Jenkin et al., 2015; Praske et al., 2015; Schwantes et al., 2015; Wennberg et al., 2018; Tsiligiannis et al., 2022 (under review)) Analysis of these multifunctional compounds is further complicated due to its secondary nature, as well as their

60   potentially long atmospheric lifetime.(Müller et al., 2014)

Isoprene nitrates are often identified as major products of isoprene oxidation. For example, studies performed in the Forschungszentrum Jülich SAPHIR chamber identified a large range of organonitrates resulting from the NO_3-initiated oxidation of isoprene, including the primary products mentioned here.(Wu et al., 2021; Brownwood et al., 2021) Chamber experiments performed at the California Institute of Technology have also highlighted the role of nitrates in the OH-initiated

65   oxidation of isoprene.(Schwantes et al., 2019; Vasquez et al., 2020) Such nitrates have also been identified in a range of ambient environments, from rural environments such as those in the south eastern United States, to polluted urban

environments such as the San Francisco Bay area.(Ayres et al., 2015; Zaveri et al., 2020) Previous modelling studies that investigate isoprene nitrates under ambient conditions, and their impacts on atmospheric chemistry, are also widespread across polluted and less polluted environments, examining both speciated nitrates and the sum of total organic nitrates.(Pratt

70   et al., 2012; Xiong et al., 2015; Romer et al., 2016; Chen et al., 2018; Zare et al., 2018; Schwantes et al., 2020)

Isoprene nitrates have also been identified as significant species during the 2017 Atmospheric Pollution and Human Health in a Chinese Megacity (APHH) summer campaign in Beijing.(Hamilton et al., 2021; Newland et al., 2021) There have been two previous box-modelling investigations focussed on the data collected during the APHH-Beijing intensive field observations.(Reeves et al., 2021; Whalley et al., 2021) Whalley *et al.* focussed on radical chemistry and ozone formation,

75   highlighting several inconsistencies between modelled radical species and relevant measurements. Reeves *et al.* investigated IHN and ICN speciation and demonstrated the value of speciated measurements of isoprene nitrates by identifying several instances where the modelled IHN isomer distribution was not consistent with their measured distribution. They also discussed issues around the simplified representations of ICN isomers with regards to the initial site of attack of NO_3 and the E/Z stereochemistry of 1,4-ICN and 4,1-ICN. This paper uses similar box-modelling approaches as the previously discussed

80   studies to assess the capabilities of three detailed atmospheric oxidation mechanisms for investigating the formation and losses of isoprene derived nitrates in this anthropogenically and biogenically impacted environment. Key statistics for each mechanism are given in Table S1.

The first mechanism used here is the Master Chemical Mechanism v3.3.1 (MCM).(Jenkin et al., 2015) The MCM is a benchmark near-explicit chemical mechanism extensively used by the atmospheric science community in a wide variety of

85   science and policy applications where chemical detail is required. Subsets of the MCM can be directly extracted for a wide variety of VOCs (mcm.york.ac.uk). However, due to the breadth of the MCM, some simplifications have been made when constructing the mechanism. The first major simplification is the use of lumped RO_2 reactions. This means that RO_2-RO_2 cross-reactions are not treated explicitly, and it is assumed that each RO_2 will react with any other RO_2 at the same rate, which helps to greatly reduce the complexity of mechanisms.(Jenkin et al., 1997) In the case of isoprene, further assumptions

90   are made. For example, NO_3-initiated oxidation of isoprene in the MCM is represented by only one isomer (NISOPO2).

Secondly, the isoprene oxidation mechanism taken from the Wennberg *et al.* 2018 review of gas-phase isoprene oxidation (henceforth, the Caltech Mechanism) was used.(Wennberg et al., 2018) This mechanism treats isoprene RO_2 cross-reactions explicitly, unlike the lumped-RO_2 approach of the MCM. This leads to issues when integrating the Caltech Mechanism with the MCM subset for additional measured VOCs, as explained further in the methodology section. The Caltech Mechanism

95   aims to provide a more up-to-date representation of reaction rates and products. For example, the Caltech Mechanism provides four different nitrated RO_2 radicals resulting from NO_3 oxidation. The Caltech Mechanism also introduces some reactions that are not found in the MCM, such as intramolecular RO_2 reactions.

Finally, the mechanism developed by Vereecken *et al.* and further expanded in Tsiligiannis *et al.* was used and is referred to as the FZJ Mechanism.(Vereecken et al., 2021; Tsiligiannis et al., 2022 (under review)) This mechanism aims to expand on

100   the Caltech Mechanism, by providing more comprehensive NO_3 chemistry, including the proposed formation of epoxide

species from some alkoxy radical species, and additional chemistry relevant to $C_4H_7NO_5$ outlined in Tsiligiannis *et al.*(Tsiligiannis et al., 2022 (under review))

2 Methodology

2.1 Ambient Measurements

105   The Beijing measurements used in this work were collected at ground level at the Tower Section of the Institute of Atmospheric Physics (IAP) in Beijing, China, between 2021-06-01 and 2021-06-18.(Shi et al., 2019) The nitrates were measured using a Filter Inlet for Gases and Aerosols (FIGAERO) coupled to a time-of-flight iodide chemical ionisation mass spectrometer (I^--CIMS) which allows for the measurement of particle and gas-phase species, although only the gas-phase data are used here as the particle-phase data were unavailable.(Lopez-Hilfiker et al., 2014) Each nitrate was calibrated

110   assuming the same sensitivity as IEPOX.(Hamilton et al., 2021) Other organic compounds were measured by proton transfer mass spectrometry (PTR-MS), selected ion flow tube mass spectrometry (SIFT-MS), comprehensive two dimensional gas chromatography with flame ionisation detection (GC×GC-FID), and dual-channel gas chromatography with flame ionization detection (DC-GC-FID).(Hopkins et al., 2011; Dunmore et al., 2015; Huang et al., 2016; Shi et al., 2019; Reeves et al., 2021) Instruments used to measure organic species are summarised in Table S2 and the details of the instruments used to

115   measure additional compounds can be found elsewhere.(Whalley et al., 2010; Whalley et al., 2018; Zhou et al., 2018; Shi et al., 2019; Hamilton et al., 2021; Whalley et al., 2021) Where species constraints were required in the modelling, and multiple measurements were taken, the mean of all of the measurements was used. The scanning mobility particle sizer (SMPS) instruments used to calculate particle surface area as outlined in the Results and Discussion section are described in the Supplementary Information.

120   **2.2 Mechanisms**

This investigation involved a comparison of three different isoprene oxidation mechanisms. The MCM subset for isoprene and the additional VOCs which were measured throughout the campaign and were available in the MCM (Table S2) was extracted directly from the MCM website (mcm.york.ac.uk).(Jenkin et al., 2015) The MCM inorganic chemistry scheme was used for all three mechanisms.

125   The Caltech Mechanism was integrated with the MCM subset for the additional VOCs by producing lumped RO_2 cross-reactions by averaging the rates of all cross-reactions for a specific RO_2 species. This approach assumes that the reaction of each isoprene RO_2 with any other RO_2 will proceed at the average rate of each isoprene RO_2 cross-reaction described in the Caltech Mechanism.

The FZJ Mechanism was produced by adding the reactions outlined in Tsiligiannis *et al.* to the mechanism provided in

130   Vereecken *et al.* and combining it with the MCM subset for measured non-isoprene species. (Vereecken et al., 2021; Tsiligiannis et al., 2022 (under review))

2.3 Modelling Approach

AtChem2, an open-source zero-dimensional box-model tool, was used in this work.(Sommariva et al., 2019) A separate model was run for each day to avoid compounding errors carrying across multiple days of the model, for example the uncertainty that may result from imperfect accounting for physical processes. NO_2, O_3, CO, SO_2, HONO, and formaldehyde, along with 40 primary VOCs for which data were available (Table S2), were all constrained to the 30-minute averaged measured values throughout the campaign. NO was left unconstrained due to the potential for local NO emissions to result in mixing ratios unrepresentative of the larger area that is important for the formation of long-lived organic products such as organonitrates. Constraining to NO would result in unrealistically low NO_3 concentrations by increasing the rate of the NO_3 + NO reaction based on elevated NO concentrations. Temperature, pressure, boundary-layer height, and relative humidity were also constrained to measured values. Photolysis values in the models were constrained to measured values where available (J_{O1D}, J_{NO2}, J_{HONO}, J_{HCHOr}, J_{HCHOnr}, $J_{NO3toNO}$, $J_{NO3toNO2}$, J_{CH3CHO}, $J_{CH3OCH3}$), and remaining photolysis rates were calculated according to the parameterization used in the MCM and scaled based on the ratio of the calculated and measured J_{NO2}. The models consisted of a 24-hour spin-up period followed by a further 24-hour period. Constraints were made by duplicating the measured values for each day to provide a 48-hour constraint of two repeated 24-hour periods. The model output was then considered to be the model output in the second 24-hour period of the model run. The model outputs were then concatenated to produce a time series across the whole period of interest.

To account for the deposition of species to surfaces, deposition reactions were added for all species. Each species was assigned a deposition velocity based on the functionality of that compound. Deposition velocities for H_2O_2, HNO_3, and O_3 were applied directly to each compound. Separate deposition velocities for organic hydroperoxides and organic nitrates were applied to compounds containing the hydroperoxide and nitrate functional groups. Organic acid species were assigned the formic acid deposition velocity, and a general oxidised VOC deposition was assigned to carbonyl and alcohol containing compounds. For multifunctional compounds, the largest deposition velocity was selected. The rate of deposition was determined by multiplying the assigned deposition velocity by the measured boundary layer height. All deposition velocities were taken from Nguyen *et al.* 2015 and are summarised in Table S3.(Nguyen et al., 2015)

Additionally, a loss term was included for all species to account for mixing and ventilation. Since the magnitude of the ventilation rate is highly uncertain, a rate of 1.157×10^{-5} s^{-1} was given for all species, resulting in a lifetime with respect to ventilation of 24 hours. The sensitivity of the model results to this term is assessed in the Model Validation section.

3 Results and Discussion

3.1 Model Validation

When comparing the measured and modelled NO mixing ratios, there is good agreement during the day-time, with the models deviating from the measurement by a maximum of around 2 times (Figure 6a). The models do not reproduce the

elevated night-time NO concentrations observed in Beijing, however this night-time NO is likely the result of local emissions and so will have little impact on the chemistry that is the focus of this study. Figure S1 shows the good match

165 between modelled NO and NO measured at an altitude of 100m showing the ability of the model to predict NO away from local sources. This is further confirmed by NO_3 predictions provided by the models being, at most, 2.5 times over-predicted (Figure 6b). There is also a slight under-prediction of NO_3 by a factor of around 0.4 during the afternoon.

HO_x predictions from the models are generally good. There is close agreement to the measured OH concentrations, although the modelled concentrations are around 0.5 times the measured values during the morning period (Figure 6c). Day-time HO_2

170 concentrations are around 2 times higher than the measurement in all models (Figure 6d), which is consistent with findings from Whalley *et al.* 2021 where a similar box-model run using the MCM over-predicted HO_2, particularly during low-NO periods. Whalley *et al.* hypothesises that the HO_2 over-prediction may be caused by unaccounted for RO isomerisation reactions that result in RO_2 radical formation without concurrent HO_2 formation.(Whalley et al., 2021) While the Caltech Mechanism and FZJ Mechanism both include additional RO isomerisation reactions for isoprene, they inherit the MCM RO

175 chemistry for other VOCs, including longer-chain VOCs that may be more susceptible to RO isomerisations, and so this could still be a reasonable hypothesis. The major contributors to RO composition in the models are aromatic species owing to their relatively long lifetimes.

When comparing the modelled and measured MVK and MACR mixing ratios, while the models are within the uncertainty of the measurements during the night, there is an over-prediction of around 3 times during the day across all models (Figure

180 S2). This is likely due to imperfect accounting for physical processes such as mixing and ventilation within the models, though there could also be contributions resulting from a poor understanding of the MVK+MACR chemistry in this environment. While a ventilation term is included in the models, there is a large uncertainty as to its true rate and diurnal variability. As a test of the models' sensitivity to the ventilation rate, the rate was halved and doubled in two separate tests (Figure S3). The halving of the ventilation rates resulted in an average change in concentration across the models run with

185 each mechanism of 15%, 6%, 8%, and 9% for $\Sigma C_4H_7NO_5$, ΣIHN, ΣICN, and ΣIPN respectively. The average changes for doubling the ventilation rate were -40%, -12%, -17%, and -19% for $\Sigma C_4H_7NO_5$, ΣIHN, ΣICN, and ΣIPN respectively. Xiong *et al.* aimed to reduce the impact of ventilation by analysing nitrates as ratios with the sum of MVK and MACR.(Xiong et al., 2015) However, due to the differences in MVK+MACR predicted using each mechanism, using the MVK+MACR ratio as a proxy for the absolute concentration of the nitrates complicates the comparison of different mechanisms. As such, the

190 analysis here primarily involves the use of mixing ratios as opposed to the ratios relative to MVK+MACR. In order to analyse the average trends over a day within the modelled period, average diurnal plots are used to examine the modelled and measured data. The mean diurnals are used here, though use of the median had little impact on the diurnal values.

Comparison of the MVK+MACR predicted using each mechanism is consistent with the work presented in Vereecken *et al.* (Vereecken et al., 2021) Figure S2 shows that the Caltech Mechanism produces the highest night-time MVK+MACR

195 concentrations with the MCM and FZJ Mechanism producing the lowest night-time concentrations. The MCM does not include MVK+MACR formation from isoprene+NO_3 chemistry, while the Caltech Mechanism does. The FZJ Mechanism

does include some MVK+MACR formation from isoprene NO_3 chemistry, but also reduces the yield from ozonolysis reactions resulting in similar MVK+MACR yields between the MCM and FZJ Mechanism in Vereecken *et al.* and in the night-time period of the models presented here. During the day-time, the FZJ models produce the lowest MVK+MACR concentrations as this adjusted ozonolysis chemistry becomes more significant.

Isoprene epoxydiols (IEPOX) are a significant contributor to isoprene-derived SOA and are significant isoprene oxidation products along with the isobaric isoprene hydroxyhydoperoxides (ISOPOOH).(Paulot et al., 2009; Surratt et al., 2010; Nguyen et al., 2014) Figure S4 shows the modelled and measured ΣIEPOX+ISOPOOH. All three mechanisms show a similar trend relative to the measurement as is seen for MVK+MACR (Figure S2), with an over-prediction of approximately 1.25 times in the afternoon and a significant under prediction in the morning. This large under-prediction in the morning may result from the under-prediction of OH in the morning period or another missing source. Since the reactive uptake of IEPOX to acidified particles is not included in these models, it seems likely that the issue is the result of an under-prediction of the formation rate of IEPOX and not an over-prediction of the losses.

The volatility of the nitrate species was assessed in order to determine the potential impact of condensation to the particle phase. An equilibrium partitioning approach was taken, as described in Mohr *et al.* 2019.(Mohr et al., 2019) This resulted in common logarithm of saturation concentrations in units of molecules cm^{-3} ($\log(C_{sat})$) of between 4.0 and 5.3, revealing the high volatility of these compounds. As such, the condensation of these nitrates to the particle phase is assumed to be negligible, though this approach does not account for reactive uptake to particles.

3.2 ΣIPN ($C_5H_9NO_5$)

The measured ΣIPN shows little diurnal variation (Figure 7). Contrary to observations, all models produced strong diurnal profiles of ΣIPN. This is because the only losses of IPN in all mechanisms, besides the added deposition reactions, are photolysis reactions and the reaction with OH, which are day-time processes, resulting in no night time loss routes. The Caltech Mechanism produces the lowest ΣIPN mixing ratios, though the strong diurnal profile results in night-time mixing ratios being over-predicted by around 1.75 times and day-time mixing ratios being around 0.25 times the measured value. Both the MCM and FZJ Mechanism result in ΣIPN reaching a minimum at sunrise, gradually increasing throughout the day, before a rapid night-time increase. The time series for modelled and measured ΣIPN is shown in Figure S5.

To understand the trends in ΣIPN, it is important to consider the multiple isomeric (non-IPN) species present in each of the mechanisms which can make up a large proportion of the modelled ΣIPN (i.e. species with the formula $C_5H_9NO_5$). The most significant isomers of IPN are C51NO3, originally from the MCM and present in all mechanisms, ISOP1N23O4OH, present in the Caltech Mechanism and FZJ Mechanism, and ISOP1N253OH4OH, present in the Caltech Mechanism (Figure S6). C51NO3 is a nitrated hydroxy carbonyl compound in the MCM with formation routes from isoprene, as well as from hydrocarbons such as pentane. In the MCM and FZJ Mechanism models, C51NO3 makes up the majority of modelled ΣIPN composition during the day-time and into the evening (Figure S7). This is the species responsible for the gradual increase in ΣIPN throughout the day in the MCM and FZJ Mechanism models. C51NO3 production from isoprene is not included in the

230 Caltech Mechanism, and so the only formation routes to C51NO3 are from non-isoprene species. As such, C51NO3 only makes a small contribution to total ΣIPN in the Caltech Mechanism model and the day-time increase is not present.

ISOP1N253OH4OH is only present in the Caltech Mechanism and is initially formed from an intramolecular H-shift of the 1,4 isoprene alkoxy nitrate (INO), ISOP1N4O. The Caltech Mechanism does not contain any loss reactions for this species, which may account for its significant contribution to modelled night-time ΣIPN (Figure S7). This INO H-shift pathway is not

235 included in the FZJ Mechanism and so ISOP1N253OH4OH is not present.

ISOP1N23O4OH is a nitrated hydroxyepoxide that was proposed, alongside other positional isomers which are produced by the models in lower amounts, as a product of IPN OH oxidation by Schwantes *et al.* where it is termed isoprene nitrooxy hydroxyepoxide (INHE).(Schwantes et al., 2015) While the formation of INHE from IPN is present in the Caltech Mechanism, epoxidation reactions from alkoxy radicals that are predicted in Vereecken *et al.* result in much more INHE

240 production in the FZJ Mechanism model. The FZJ Mechanism model results predict that at midnight, around half of the total ΣIPN is composed of INHE (Figure 8). If such large concentrations of these epoxides are produced, then this could have a significant impact on SOA formation via reactive uptake in a similar fashion to IEPOX.(Paulot et al., 2009; Surratt et al., 2010; Schwantes et al., 2015; Hamilton et al., 2021)

In order to assess the potential for reactive uptake of INHE to bring the modelled ΣIPN in line with measurements, loss

245 reactions for each of the four INHE isomers in the FZJ Mechanism were added to the mechanism and the models rerun. The rate coefficient for the reactive uptake of INHE (k_{INHE}) was calculated using Equation 1, where S_a is the aerosol surface area, as calculated for each model time-step from scanning mobility particle sizer (SMPS) measurements, r_p is the effective particle radius calculated as a weighted median of the SMPS number measurements at each model time-step, D_g is the gas-phase diffusion coefficient, v is the mean molecular speed of INHE molecules in the gas phase, and γ_{INHE} is the reactive

250 uptake coefficient of INHE. v was calculated using Equation 2 where R is the ideal gas constant (8.314 J K^{-1} mol^{-1}), T is the measured temperature at each time-step, and M_r is the molecular mass of INHE (0.16313 kg mol^{-1}). A value of 1×10^{-5} m^2 s^{-1} was used for D_g, as is assumed in Gaston *et al.* for IEPOX. (Gaston et al., 2014) This method has been extensively used to calculate the rate of reactive uptake of IEPOX. (Gaston et al., 2014; Riedel et al., 2016; Budisulistiorini et al., 2017)

$$k_{INHE} = \frac{S_a}{\frac{r_p}{D_g} + \frac{4}{v\,\gamma_{INHE}}} \qquad\qquad Equation\ 1$$

$$v = \sqrt{\frac{3\,R\,T}{M_r}} \qquad\qquad Equation\ 2$$

255 An estimation of γ_{INHE} is complicated by the dependence on particle properties, but Figure S8 shows the modelled ΣIPN produced by a range of models for which a range of γ_{INHE} were assumed, between the limits of 0 and 1. When $\gamma_{INHE}=1$ and $\gamma_{INHE}=0.1$, almost all of the INHE is removed from the gas-phase at any time which brings the modelled night-time concentrations of ΣIPN closer to the measured value, though there is still an over-prediction of around 2 times in the early night-time. When $\gamma_{INHE} = 0.01$, the modelled night-time ΣIPN is close to the modelled value when $\gamma_{INHE} = 1$, whereas a γ_{INHE}

260   of 0.001 results in modelled concentrations close to the values without any particle uptake. Previous estimations of the
        reactive uptake coefficient of IEPOX (γ_{IEPOX}) usually range between 7×10^{-2} and 2×10^{-4}, though measurements have been
        made as low as 9×10^{-7}. (Gaston et al., 2014; Riedel et al., 2015; Budisulistiorini et al., 2017) As such, it is unlikely that the
        reactive uptake of INHE can explain the over prediction in night-time ΣIPN made by the FZJ model.

3.3 ΣIHN ($C_5H_9NO_4$)

265   Throughout the day, the three mechanisms produce similar ΣIHN mixing ratios, at approximately twice the measured value.
        Despite the absolute differences, the profile of modelled ΣIHN matches the measurement, with decreasing mixing ratios in
        the afternoon reflecting the titration of NO by increasing O_3.(Newland et al., 2021) The largest deviation between the models
        occurs at night, where the Caltech Mechanism produces a night-time peak in ΣIHN which is not observed in the other
        models or the measurements (Figure 9). Furthermore, ΣIHN concentrations fall rapidly through the early morning in the
270   MCM and Caltech Mechanism models while the FZJ Mechanism model is more consistent with the profile of the
        measurements as the ΣIHN mixing ratio remains stable between 00:00 and 06:00. Reeves *et al.* shows reasonable predictions
        of 1,2-IHN made by their MCM-based model, however the modelled 4,3-IHN showed a similar trend to the ΣIHN from the
        MCM model shown here, with an over-prediction of around two times at mid-day.(Reeves et al., 2021) The time series for
        modelled and measured ΣIHN is shown in Figure S9.

275   Figure 10 shows the clear split between the day-time and night-time IHN speciation in all of the models. Figure 10 also
        demonstrates that the contribution of non-IHN species to ΣIHN in the models is very small, meaning a measured ΣIHN
        ($C_5H_9NO_4$) signal is likely to be a reasonable measurement of IHN. Both OH and NO_3 addition to isoprene favours the
        terminal carbon atoms, so OH oxidation followed by reaction with NO results in the nitrate group being formed either on one
        of the central positions or the remaining terminal carbon. This means OH-initiated oxidation predominantly forms 1,2-IHN,
280   4,3-IHN, E/Z-1,4-IHN, and E/Z-4,1-IHN. NO_3 addition results in the nitrate group being present on the terminal carbons, at
        the initial site of attack.(Wennberg et al., 2018) This means NO_3-initiated oxidation predominantly forms 2,1-IHN, 3,4-IHN,
        E/Z-1,4-IHN, and E/Z-4,1-IHN.

        The night-time shows an enhancement in IHN species produced by NO_3 chemistry. This is most obvious in the MCM model,
        where all isoprene + NO_3 chemistry is channelled through just one isomer, ISOPCNO3. As such, ISOPCNO3 makes up very
285   little of the day-time IHN, but up to 80% of night-time IHN just before sunrise. Similarly, the ΣIHN modelled using the
        Caltech Mechanism and FZJ Mechanism are almost exclusively comprised of ISOP1OH2N and ISOP3N4OH during the
        day, but there is a more even distribution at night with major contributions from ISOP1N2OH, ISOP1N4OHt, and
        ISOP1N4OHc. The FZJ Mechanism contains a reduced rate of ISOP1N2OH formation from ISOP1N2OO cross-reactions
        compared to the Caltech Mechanism, hence the far lower contribution of 'NO₃-initiated IHN' to ΣIHN in the FZJ
290   Mechanism model. This also helps to explain the elevated absolute night-time ΣIHN concentrations observed when using the
        Caltech Mechanism compared to using the FZJ Mechanism (Figure 9).

This composition difference offers potential for identifying the source of oxidation for isoprene impacted air masses. An air mass dominated by 1,2- and 4,3-IHN likely results from OH oxidation, though differing rates of hydrolysis between IHN isomers would also alter this distribution.

295 Additionally, recognising this changing IHN composition profile could aid with the calibration of instruments that cannot distinguish between IHN isomers. The instrument response of an IHN measurement which cannot distinguish isomers necessitates an assumption as to the expected isomer distribution, since each ΣIHN isomer will have a different response. Ideally, some consideration will be given to the different sensitivities of the instrument to different isomers.(Lee et al., 2014) However, it is difficult to obtain authentic standards for many of the species of interest. It has been previously shown that I^--

300 CIMS is more sensitive to IHN isomers in which the NO_3 group is located close to the OH group, such as 4,3-IHN and Z-1,4-IHN. Isomers where the NO_3 and OH groups are not in close proximity, such as E-1,4-IHN, show much lower responses to iodide-adduct ionisation. (Lee et al., 2014)   While it may be convenient to assume a constant IHN ratio distribution governed by that expected from OH oxidation, the recognition of changing IHN sources over the course of 24-hours implies the requirement for a varying calibration factor. The "Mixed-source IHN" in Figure 10 includes E and Z isomers of 1,4-IHN

305 and 4,1-IHN. Since there is a higher proportion of mixed-source IHN during the night in all models, the response factor of ΣIHN can be expected to be lower at night than during the day due to a higher proportion of E-1,4-IHN and E-4,1-IHN. This varying calibration factor may help to explain the perceived over-prediction of ΣIHN during the night-time made by all models, due to the artificially supressed ΣIHN signal resulting from the use of a constant calibration factor.

3.4 ΣICN ($C_5H_7NO_4$)

310 ΣICN shows the largest difference between mechanisms. In line with the measurements, all models show low concentrations of ΣICN during the day (Figure 11). ΣICN then increases at sunset, due to NO_3-initiated formation from isoprene, and then reduces in concentration into the early morning as production ceases. There is a large over-prediction of a factor of ≈35 times in the night-time mixing ratio modelled using the MCM which is consistent with findings from Reeves *et al.* who also found ICN to be over-predicted in their models using the MCM, however the lack of NO constraint in our models results in higher

315 modelled ICN concentrations due to elevated NO_3 concentrations, hence the discrepancy between the model and measurement is larger in this work.(Reeves et al., 2021) This over-prediction decreases to around 10 times when using the Caltech Mechanism, and decreases further to around 4 times when using the FZJ Mechanism. A plot of ΣICN concentrations normalised to the concentration at midnight is shown in Figure S10. The time series for measured and modelled ΣICN is given in Figure S11. It is also important to consider that previous work has found the lower sensitivity to aldehyde and

320 ketone groups by I^--CIMS compared to alcohols, as such it should be expected that the measured ΣICN is most likely to be under-quantified by use of the IEPOX calibrant compared to species such as IHN.(Lopez-Hilfiker et al., 2014; Iyer et al., 2016)

The large over-prediction made by the MCM is the result of large production terms from the decomposition of all INO radicals (represented by NISOPO in the MCM) into ICN. In contrast, the Caltech Mechanism provides alternative INO

325 decomposition routes including fragmentation and H-shift autoxidation reactions (Figure S12). The FZJ Mechanism includes much of this updated chemistry as well as proposing the previously discussed epoxide formation reactions from some alkoxy radicals, which further reduces the ICN production route (Figure S12). The improvement in predictions of ΣICN indicates that the assumption made by the MCM of 100% of INO decomposing to form ICN is unlikely to be valid. The loss of ΣICN is dominated by physical processes in all of the models, particularly at night when ΣICN concentrations are the highest.

330 Additional ICN losses being added to the MCM may improve ΣICN predictions, for example Hamilton *et al.* proposed ICN as a precursor to particle-phase species observed in Beijing via an isoprene nitrooxy hydroxy-α-lactone (INHL) species.(Hamilton et al., 2021) However, the MCM already includes reactions with O_3 and NO_3 that are not included in the Caltech or FZJ Mechanisms, suggesting that the issue lies in the MCM's faster formation processes. Further discussion of the uncertainties in ICN losses is given by Reeves *et al.*(Reeves et al., 2021)

335 **3.5 $\Sigma C_4H_7NO_5$**

Day-time $\Sigma C_4H_7NO_5$ mixing ratios are over-predicted in all models, while night-time mixing ratios are approximately in line with measurements (Figure 12a). This is broadly consistent with the differences between measured and modelled MVK and MACR (Figure S2). Since the models show that most of the $C_4H_7NO_5$ is formed during the day from MVK and MACR, analysing the $\Sigma C_4H_7NO_5$/(MVK+MACR) ratio will allow for the influence of the MVK+MACR over-prediction to be

340 minimised (Figure 12b). This is distinct from the use of MVK+MACR ratios used by Xiong *et al.* where the purpose was to minimise the impact of uncertainties in the rates of physical processes.(Xiong et al., 2015) The $\Sigma C_4H_7NO_5$/(MVK+MACR) diurnals only slightly vary between each model. While the $\Sigma C_4H_7NO_5$/(MVK+MACR) in the models generally matches the measured ratio well, they show slightly stronger diurnal variation than is observed in the measurement, where the ratio remains relatively constant throughout the day. The time series for measured and modelled $\Sigma C_4H_7NO_5$ and

345 $\Sigma C_4H_7NO_5$/(MVK+MACR) is given in Figure S13 and Figure S14.

The results indicate that the formation of $C_4H_7NO_5$ from MVK and MACR, primarily through OH reaction pathways, is reasonably well represented in existing chemical mechanisms.

4 Conclusions

Model results have been presented making use of three different detailed chemical mechanisms, comparing their predictions

350 of several isoprene organonitrates. While the gas-phase box-modelling approach used here allows for the use of such complex mechanisms, the simplified representation may not fully represent physical processes such as boundary layer mixing in the morning and evening. Additionally, hydrolysis and aerosol uptake processes are not included in the mechanisms, meaning there may be unaccounted losses for species such as INHE. Additionally, the measurement techniques potentially have significant issues with calibration factors, which can change over the course of a day as isomer composition

355 changes. The availability of authentic standards would greatly improve the ability to quantify such organonitrates.

When considering ΣIPN, the model results presented here indicate that large proportions of the measured ΣIPN can be composed of non-IPN species. This is especially true during the daytime, when ΣIPN concentrations are lowest. However, the epoxide-forming reactions proposed by Vereecken *et al.* suggest that around half of the measured night-time ΣIPN could be comprised of INHE.(Vereecken et al., 2021) Assuming reactive uptake coefficients similar to those previously measured for IEPOX results in small reductions in predicted ΣIPN, indicating that reactive uptake of INHE cannot fully explain the over prediction of ΣIPN made when using the FZJ mechanism. Further studies of isoprene nitrate chemistry should investigate these species with techniques able to distinguish between the isomeric ΣIPN compounds and their reaction products, such as chromatographic techniques, in order to determine the role of INHE in isoprene oxidation. Such large INHE production terms would have implications for the formation and growth of secondary organic aerosol (SOA) by reactive uptake to acidified particles.(Hamilton et al., 2021) Generally, the large contribution of non-IPN species to the modelled ΣIPN highlights the caution that should be applied in interpreting measurements of ΣIPN solely as a measurement of IPN.

The changing distribution of ΣIHN isomers over the course of 24-hours has implications for the calibration of ΣIHN measurements. For example, I$^-$-CIMS will be less sensitive to IHN overnight where NO$_3$ chemistry is dominant, due to the increased contribution of E-1,4-IHN and E-4,1-IHN to ΣIHN. This means that the use of a constant calibration factor is likely to under-quantify night-time IHN, even if the calibration factor was accurate during the day.

The much improved ΣICN predictions when using the Caltech and FZJ Mechanisms compared to the MCM indicates that the assumptions around alkoxy radical decomposition made by the MCM are likely to be inaccurate. Future studies focussed on isoprene nitrates should not overlook the inclusion of more complex INO decomposition routes, beyond the direct decomposition route to ICN present in the MCM.

When considering C$_4$H$_7$NO$_5$ species, all of the mechanisms reproduce ΣC$_4$H$_7$NO$_5$/(MVK+MACR) well, indicating the good representation of C$_4$H$_7$NO$_5$ chemistry, at least when the majority of the formation is resulting from MVK and MACR. Additional C$_4$H$_7$NO$_5$ from NO$_3$ chemistry, as is included in the FZJ Mechanism model, does not improve predictions as the majority of the modelled C$_4$H$_7$NO$_5$ resulted from OH chemistry.

The models generally predicted the concentrations of the four groups of isoprene-derived organic nitrates well, and the improvements made by the inclusion of updated nitrate chemistry highlights the advances in the understanding of isoprene nitrate chemistry made in recent years. However, the work presented here illustrates some important remaining uncertainties surrounding the prediction of night-time concentrations of IPN, ICN, and IHN.

Author Contributions

A.W.M performed the model simulations and prepared the manuscript. P.M.E and J.F.H provided supervision and advice throughout the project. B.H.L and J.A.T provided advice and feedback on the representation of isoprene nitrates in box-models and their measurement. A.R.R and B.S.N assisted in constructing the modelling approach and advised on the use of

chemical mechanisms. T.J.B, J.B, J.R.H, J.D.L, C.P, and M.D.S carried out the measurements of species used for model constraints. All authors provided feedback on early drafts of the manuscript.

Competing interests

The authors declare that they have no conflict of interest.

Acknowledgements

The authors acknowledge the support from Pingqing Fu, Zifa Wang, Jie Li, and Yele Sun from IAP for hosting the APHH Beijing campaign at IAP. They also thank Tuan Vu, Roy Harrison, Di Liu, and Bill Bloss from the University of Birmingham; Alastair Lewis, William Dixon, Marvin Shaw, and Stefan Swift from the University of York. Siyao Yue, Liangfang Wei, Hong Ren, Qiaorong Xie, Wanyu Zhao, Linjie Li, Ping Li, Shengjie Hou, and Qingqing Wang from IAP; Kebin He and Xiaoting Chen from Tsinghua University, and James Allan from the University of Manchester for providing logistic and scientific support for the field campaigns.

Financial Support

This work was supported by the Leeds-York-Hull Natural Environment Research Council

(NERC) Doctoral Training Partnership (DTP) Panorama under grant NE/S007458/1. The APHH Beijing campaign was supported by the Natural Environment Research Council (NERC) under grant NE/N006917/1.

References

Ayres, B. R., Allen, H. M., Draper, D. C., Brown, S. S., Wild, R. J., Jimenez, J. L., Day, D. A., Campuzano-Jost, P., Hu, W., de Gouw, J., Koss, A., Cohen, R. C., Duffey, K. C., Romer, P., Baumann, K., Edgerton, E., Takahama, S., Thornton, J. A., Lee, B. H., Lopez-Hilfiker, F. D., Mohr, C., Wennberg, P. O., Nguyen, T. B., Teng, A., Goldstein, A. H., Olson, K., and Fry, J. L.: Organic nitrate aerosol formation via NO3 + biogenic volatile organic compounds in the southeastern United States, Atmospheric Chemistry and Physics, 15, 13377-13392, 10.5194/acp-15-13377-2015, 2015.

Bates, K. H. and Jacob, D. J.: A new model mechanism for atmospheric oxidation of isoprene: global effects on oxidants, nitrogen oxides, organic products, and secondary organic aerosol, Atmospheric Chemistry and Physics, 19, 9613-9640, 10.5194/acp-19-9613-2019, 2019.

Brownwood, B., Turdziladze, A., Hohaus, T., Wu, R., Mentel, T. F., Carlsson, P. T. M., Tsiligiannis, E., Hallquist, M., Andres, S., Hantschke, L., Reimer, D., Rohrer, F., Tillmann, R., Winter, B., Liebmann, J., Brown, S. S., Kiendler-Scharr, A., Novelli, A., Fuchs, H., and Fry, J. L.: Gas-Particle Partitioning and SOA Yields of Organonitrate Products from NO3-Initiated Oxidation of Isoprene under Varied Chemical Regimes, ACS Earth Space Chem, 5, 785-800, 10.1021/acsearthspacechem.0c00311, 2021.

Budisulistiorini, S. H., Nenes, A., Carlton, A. G., Surratt, J. D., McNeill, V. F., and Pye, H. O. T.: Simulating Aqueous-Phase Isoprene-Epoxydiol (IEPOX) Secondary Organic Aerosol Production During the 2013 Southern
420 Oxidant and Aerosol Study (SOAS), Environmental Science & Technology, 51, 5026-5034, 10.1021/acs.est.6b05750, 2017.

Chen, X., Wang, H., and Lu, K.: Simulation of organic nitrates in Pearl River Delta in 2006 and the chemical impact on ozone production, Science China Earth Sciences, 61, 228-238, 10.1007/s11430-017-9115-5, 2018.

Dunmore, R. E., Hopkins, J. R., Lidster, R. T., Lee, J. D., Evans, M. J., Rickard, A. R., Lewis, A. C., and Hamilton, J.
425 F.: Diesel-related hydrocarbons can dominate gas phase reactive carbon in megacities, Atmospheric Chemistry and Physics, 15, 9983-9996, 10.5194/acp-15-9983-2015, 2015.

Emmerson, K. L. and Evans, M. J.: Comparison of tropospheric gas-phase chemistry schemes for use within global models, Atmos. Chem. Phys, 9, 1831-1845, https://doi.org/10.5194/acp-9-1831-2009, 2009.

Gaston, C. J., Riedel, T. P., Zhang, Z., Gold, A., Surratt, J. D., and Thornton, J. A.: Reactive Uptake of an Isoprene-
430 Derived Epoxydiol to Submicron Aerosol Particles, Environmental Science & Technology, 48, 11178-11186, 10.1021/es5034266, 2014.

Guenther, A., Karl, T., Harley, P., Wiedinmyer, C., Palmer, P. I., and Geron, C.: Estimates of global terrestrial isoprene emissions using MEGAN (Model of Emissions of Gases and Aerosols from Nature), Atmospheric Chemistry and Physics, 6, 3181-3210, 2006.

435 Guenther, A., Hewitt, C. N., Erickson, D., Fall, R., Geron, C., Graedel, T., Harley, P., Klinger, L., Lerdau, M., McKay, W. A., Pierce, T., Scholes, B., Steinbrecher, R., Tallamraju, R., Taylor, J., and Zimmerman, P.: A global model of natural volatile organic compound emissions, Journal of Geophysical Research, 100, 10.1029/94jd02950, 1995.

Guenther, A. B., Jiang, X., Heald, C. L., Sakulyanontvittaya, T., Duhl, T., Emmons, L. K., and Wang, X.: The Model of Emissions of Gases and Aerosols from Nature version 2.1 (MEGAN2.1): an extended and updated framework
440 for modeling biogenic emissions, Geoscientific Model Development, 5, 1471-1492, 10.5194/gmd-5-1471-2012, 2012.

Hamilton, J. F., Bryant, D. J., Edwards, P. M., Ouyang, B., Bannan, T. J., Mehra, A., Mayhew, A. W., Hopkins, J. R., Dunmore, R. E., Squires, F. A., Lee, J. D., Newland, M. J., Worrall, S. D., Bacak, A., Coe, H., Percival, C., Whalley, L. K., Heard, D. E., Slater, E. J., Jones, R. L., Cui, T., Surratt, J. D., Reeves, C. E., Mills, G. P., Grimmond, S., Sun, Y., Xu,
445 W., Shi, Z., and Rickard, A. R.: Key Role of NO3 Radicals in the Production of Isoprene Nitrates and Nitrooxyorganosulfates in Beijing, Environ Sci Technol, 55, 842-853, 10.1021/acs.est.0c05689, 2021.

Hopkins, J. R., Jones, C. E., and Lewis, A. C.: A dual channel gas chromatograph for atmospheric analysis of volatile organic compounds including oxygenated and monoterpene compounds, J Environ Monit, 13, 2268-2276, 10.1039/c1em10050e, 2011.

450 Huang, Z., Zhang, Y., Yan, Q., Zhang, Z., and Wang, X.: Real-time monitoring of respiratory absorption factors of volatile organic compounds in ambient air by proton transfer reaction time-of-flight mass spectrometry, J Hazard Mater, 320, 547-555, 10.1016/j.jhazmat.2016.08.064, 2016.

Iyer, S., Lopez-Hilfiker, F., Lee, B. H., Thornton, J. A., and Kurtén, T.: Modeling the Detection of Organic and Inorganic Compounds Using Iodide-Based Chemical Ionization, The Journal of Physical Chemistry A, 120, 576-
455 587, 10.1021/acs.jpca.5b09837, 2016.

Jenkin, M. E., Saunders, S. M., and Pilling, M. J.: The Tropospheric Degradation of Volatile Organic Compounds: A Protocol for Mechanism Development, Atmospheric Environment, 81-104, https://doi.org/10.1016/S1352-2310(96)00105-7, 1997.

Jenkin, M. E., Young, J. C., and Rickard, A. R.: The MCM v3.3.1 degradation scheme for isoprene, Atmospheric
460 Chemistry and Physics, 15, 11433-11459, 10.5194/acp-15-11433-2015, 2015.

Lee, B. H., Lopez-Hilfiker, F. D., Mohr, C., Kurten, T., Worsnop, D. R., and Thornton, J. A.: An iodide-adduct high-resolution time-of-flight chemical-ionization mass spectrometer: application to atmospheric inorganic and organic compounds, Environ Sci Technol, 48, 6309-6317, 10.1021/es500362a, 2014.

465 Lopez-Hilfiker, F. D., Mohr, C., Ehn, M., Rubach, F., Kleist, E., Wildt, J., Mentel, T. F., Lutz, A., Hallquist, M., Worsnop, D., and Thornton, J. A.: A novel method for online analysis of gas and particle composition: description and evaluation of a Filter Inlet for Gases and AEROsols (FIGAERO), Atmospheric Measurement Techniques, 7, 983-1001, 10.5194/amt-7-983-2014, 2014.

Mohr, C., Thornton, J. A., Heitto, A., Lopez-Hilfiker, F. D., Lutz, A., Riipinen, I., Hong, J., Donahue, N. M., Hallquist, M., Petäjä, T., Kulmala, M., and Yli-Juuti, T.: Molecular identification of organic vapors driving

470 atmospheric nanoparticle growth, Nature Communications, 10, 10.1038/s41467-019-12473-2, 2019.

Müller, J. F., Peeters, J., and Stavrakou, T.: Fast photolysis of carbonyl nitrates from isoprene, Atmospheric Chemistry and Physics, 14, 2497-2508, 10.5194/acp-14-2497-2014, 2014.

Newland, M. J., Bryant, D. J., Dunmore, R. E., Bannan, T. J., Acton, W. J. F., Langford, B., Hopkins, J. R., Squires, F. A., Dixon, W., Drysdale, W. S., Ivatt, P. D., Evans, M. J., Edwards, P. M., Whalley, L. K., Heard, D. E., Slater, E. J.,

475 Woodward-Massey, R., Ye, C., Mehra, A., Worrall, S. D., Bacak, A., Coe, H., Percival, C. J., Hewitt, C. N., Lee, J. D., Cui, T., Surratt, J. D., Wang, X., Lewis, A. C., Rickard, A. R., and Hamilton, J. F.: Low-NO atmospheric oxidation pathways in a polluted megacity, Atmospheric Chemistry and Physics, 21, 1613-1625, 10.5194/acp-21-1613-2021, 2021.

Nguyen, T. B., Crounse, J. D., Teng, A. P., St. Clair, J. M., Paulot, F., Wolfe, G. M., and Wennberg, P. O.: Rapid

480 deposition of oxidized biogenic compounds to a temperate forest, Proceedings of the National Academy of Sciences, 112, E392-E401, 10.1073/pnas.1418702112, 2015.

Nguyen, T. B., Coggon, M. M., Bates, K. H., Zhang, X., Schwantes, R. H., Schilling, K. A., Loza, C. L., Flagan, R. C., Wennberg, P. O., and Seinfeld, J. H.: Organic aerosol formation from the reactive uptake of isoprene epoxydiols (IEPOX) onto non-acidified inorganic seeds, Atmospheric Chemistry and Physics, 14, 3497-3510, 10.5194/acp-

485 14-3497-2014, 2014.

Novelli, A., Cho, C., Fuchs, H., Hofzumahaus, A., Rohrer, F., Tillmann, R., Kiendler-Scharr, A., Wahner, A., and Vereecken, L.: Experimental and theoretical study on the impact of a nitrate group on the chemistry of alkoxy radicals, Phys Chem Chem Phys, 23, 5474-5495, 10.1039/d0cp05555g, 2021.

Palmer, P. I., Marvin, M. R., Siddans, R., Kerridge, B. J., and Moore, D. P.: Nocturnal survival of isoprene linked to

490 formation of upper tropospheric organic aerosol, Science, 375, 562-566, 10.1126/science.abg4506, 2022.

Paulot, F., Crounse, J. D., Kjaergaard, H. G., Kürten, A., St Clair, J. M., Seinfeld, J. H., and Wennberg, P. O.: Unexpected Epoxide Formation in the Gas-Phase Photooxidation of Isoprene, Science, 325, 730-733, 10.1126/science.1172910, 2009.

Praske, E., Crounse, J. D., Bates, K. H., Kurten, T., Kjaergaard, H. G., and Wennberg, P. O.: Atmospheric fate of

495 methyl vinyl ketone: peroxy radical reactions with NO and HO2, J Phys Chem A, 119, 4562-4572, 10.1021/jp5107058, 2015.

Pratt, K. A., Mielke, L. H., Shepson, P. B., Bryan, A. M., Steiner, A. L., Ortega, J., Daly, R., Helmig, D., Vogel, C. S., Griffith, S., Dusanter, S., Stevens, P. S., and Alaghmand, M.: Contributions of individual reactive biogenic volatile organic compounds to organic nitrates above a mixed forest, Atmospheric Chemistry and Physics, 12, 10125-

500 10143, 10.5194/acp-12-10125-2012, 2012.

Reeves, C. E., Mills, G. P., Whalley, L. K., Acton, W. J. F., Bloss, W. J., Crilley, L. R., Grimmond, S., Heard, D. E., Hewitt, C. N., Hopkins, J. R., Kotthaus, S., Kramer, L. J., Jones, R. L., Lee, J. D., Liu, Y., Ouyang, B., Slater, E., Squires, F., Wang, X., Woodward-Massey, R., and Ye, C.: Observations of speciated isoprene nitrates in Beijing:

implications for isoprene chemistry, Atmospheric Chemistry and Physics, 21, 6315-6330, 10.5194/acp-21-6315-
505   2021, 2021.
Riedel, T. P., Lin, Y. H., Zhang, Z., Chu, K., Thornton, J. A., Vizuete, W., Gold, A., and Surratt, J. D.: Constraining
condensed-phase formation kinetics of secondary organic aerosol components from isoprene epoxydiols,
Atmos. Chem. Phys, 16, 1245-1254, 10.5194/acpd-15-28289-2015, 2016.
Riedel, T. P., Lin, Y.-H., Budisulistiorini, S. H., Gaston, C. J., Thornton, J. A., Zhang, Z., Vizuete, W., Gold, A., and
510   Surratt, J. D.: Heterogeneous Reactions of Isoprene-Derived Epoxides: Reaction Probabilities and Molar
Secondary Organic Aerosol Yield Estimates, Environmental Science & Technology Letters, 2, 38-42,
10.1021/ez500406f, 2015.
Romer, P. S., Duffey, K. C., Wooldridge, P. J., Allen, H. M., Ayres, B. R., Brown, S. S., Brune, W. H., Crounse, J. D.,
De Gouw, J., Draper, D. C., Feiner, P. A., Fry, J. L., Goldstein, A. H., Koss, A., Misztal, P. K., Nguyen, T. B., Olson, K.,
515   Teng, A. P., Wennberg, P. O., Wild, R. J., Zhang, L., and Cohen, R. C.: The lifetime of nitrogen oxides in an
isoprene-dominated forest, Atmospheric Chemistry and Physics, 16, 7623-7637, 10.5194/acp-16-7623-2016,
2016.
Schwantes, R. H., Charan, S. M., Bates, K. H., Huang, Y., Nguyen, T. B., Mai, H., Kong, W., Flagan, R. C., and
Seinfeld, J. H.: Low-volatility compounds contribute significantly to isoprene secondary organic aerosol (SOA)
520   under high-NOx conditions, Atmospheric Chemistry and Physics, 19, 7255-7278, 10.5194/acp-19-7255-2019,
2019.
Schwantes, R. H., Teng, A. P., Nguyen, T. B., Coggon, M. M., Crounse, J. D., St. Clair, J. M., Zhang, X., Schilling, K.
A., Seinfeld, J. H., and Wennberg, P. O.: Isoprene NO3 Oxidation Products from the RO2 + HO2 Pathway, Journal
of Physical Chemistry A, 119, 10158-10171, 10.1021/acs.jpca.5b06355, 2015.
525   Schwantes, R. H., Emmons, L. K., Orlando, J. J., Barth, M. C., Tyndall, G. S., Hall, S. R., Ullmann, K., St. Clair, J. M.,
Blake, D. R., Wisthaler, A., and Bui, T. P. V.: Comprehensive isoprene and terpene gas-phase chemistry improves
simulated surface ozone in the southeastern US, Atmospheric Chemistry and Physics, 20, 3739-3776,
10.5194/acp-20-3739-2020, 2020.
Shi, Z., Vu, T., Kotthaus, S., Harrison, R. M., Grimmond, S., Yue, S., Zhu, T., Lee, J., Han, Y., Demuzere, M.,
530   Dunmore, R. E., Ren, L., Liu, D., Wang, Y., Wild, O., Allan, J., Acton, W. J., Barlow, J., Barratt, B., Beddows, D.,
Bloss, W. J., Calzolai, G., Carruthers, D., Carslaw, D. C., Chan, Q., Chatzidiakou, L., Chen, Y., Crilley, L., Coe, H.,
Dai, T., Doherty, R., Duan, F., Fu, P., Ge, B., Ge, M., Guan, D., Hamilton, J. F., He, K., Heal, M., Heard, D., Hewitt,
C. N., Hollaway, M., Hu, M., Ji, D., Jiang, X., Jones, R., Kalberer, M., Kelly, F. J., Kramer, L., Langford, B., Lin, C.,
Lewis, A. C., Li, J., Li, W., Liu, H., Liu, J., Loh, M., Lu, K., Lucarelli, F., Mann, G., McFiggans, G., Miller, M. R., Mills,
535   G., Monk, P., Nemitz, E., O'Connor, F., Ouyang, B., Palmer, P. I., Percival, C., Popoola, O., Reeves, C., Rickard, A.
R., Shao, L., Shi, G., Spracklen, D., Stevenson, D., Sun, Y., Sun, Z., Tao, S., Tong, S., Wang, Q., Wang, W., Wang, X.,
Wang, X., Wang, Z., Wei, L., Whalley, L., Wu, X., Wu, Z., Xie, P., Yang, F., Zhang, Q., Zhang, Y., Zhang, Y., and
Zheng, M.: Introduction to the special issue "In-depth study of air pollution sources and processes within Beijing
and its surrounding region (APHH-Beijing)", Atmospheric Chemistry and Physics, 19, 7519-7546, 10.5194/acp-
540   19-7519-2019, 2019.
Sindelarova, K., Granier, C., Bouarar, I., Guenther, A., Tilmes, S., Stavrakou, T., Müller, J. F., Kuhn, U., Stefani, P.,
and Knorr, W.: Global data set of biogenic VOC emissions calculated by the MEGAN model over the last 30
years, Atmospheric Chemistry and Physics, 14, 9317-9341, 10.5194/acp-14-9317-2014, 2014.
Sommariva, R., Cox, S., Martin, C., Borońska, K., Young, J., Jimack, P., Pilling, M. J., Matthaios, V. N., Newland, M.
545   J., Panagi, M., Bloss, W. J., Monks, P. S., and Rickard, A. R.: AtChem, an open source box-model for the Master
Chemical Mechanism, Geoscientific Model Development, 10.5194/gmd-2019-192, 2019.

Surratt, J. D., Chan, A. W. H., Eddingsaas, N. C., Chan, M., Loza, C. L., Kwan, A. J., Hersey, S. P., Flagan, R. C., Wennberg, P. O., and Seinfeld, J. H.: Reactive intermediates revealed in secondary organic aerosol formation from isoprene, Proceedings of the National Academy of Sciences, 107, 6640-6645, 10.1073/pnas.0911114107, 2010.

Tsiligiannis, E., Wu, R., Lee, B. H., Garcia Salvador, C. M., Priestley, M., Carlsson, P. T. M., Kang, S., Novelli, A., Vereecken, L., Fuchs, H., Mayhew, A. W., Hamilton, J. F., Edwards, P. M., Fry, J. L., Brownwood, B., Brown, S. S., Wild, R. J., Bannan, T. J., Coe, H., Allan, J., Surratt, J. D., Bacak, A., Artaxo, P., Percival, C., Guo, S., Hu, M., Wang, T., Mentel, T. F., Thornton, J. A., and Hallquist, M.: A four carbon organonitrate as a significant product of secondary isoprene chemistry, Geophys. Res. Lett., 2022 (under review).

Vasquez, K. T., Crounse, J. D., Schulze, B. C., Bates, K. H., Teng, A. P., Xu, L., Allen, H. M., and Wennberg, P. O.: Rapid hydrolysis of tertiary isoprene nitrate efficiently removes NOx from the atmosphere, Proc Natl Acad Sci U S A, 117, 33011-33016, 10.1073/pnas.2017442117, 2020.

Vereecken, L., Carlsson, P. T. M., Novelli, A., Bernard, F., Brown, S. S., Cho, C., Crowley, J. N., Fuchs, H., Mellouki, W., Reimer, D., Shenolikar, J., Tillmann, R., Zhou, L., Kiendler-Scharr, A., and Wahner, A.: Theoretical and experimental study of peroxy and alkoxy radicals in the NO3-initiated oxidation of isoprene, Phys Chem Chem Phys, 23, 5496-5515, 10.1039/d0cp06267g, 2021.

Wennberg, P. O., Bates, K. H., Crounse, J. D., Dodson, L. G., McVay, R. C., Mertens, L. A., Nguyen, T. B., Praske, E., Schwantes, R. H., Smarte, M. D., St Clair, J. M., Teng, A. P., Zhang, X., and Seinfeld, J. H.: Gas-Phase Reactions of Isoprene and Its Major Oxidation Products, Chemical Reviews, 118, 3337-3390, 10.1021/acs.chemrev.7b00439, 2018.

Whalley, L. K., Stone, D., Dunmore, R., Hamilton, J., Hopkins, J. R., Lee, J. D., Lewis, A. C., Williams, P., Kleffmann, J., Laufs, S., Woodward-Massey, R., and Heard, D. E.: Understanding in situ ozone production in the summertime through radical observations and modelling studies during the Clean air for London project (ClearfLo), Atmospheric Chemistry and Physics, 18, 2547-2571, 10.5194/acp-18-2547-2018, 2018.

Whalley, L. K., Furneaux, K. L., Goddard, A., Lee, J. D., Mahajan, A., Oetjen, H., Read, K. A., Kaaden, N., Carpenter, L. J., Lewis, A. C., Plane, J. M. C., Saltzman, E. S., Wiedensohler, A., and Heard, D. E.: The chemistry of OH and HO2 radicals in the boundary layer over the tropical Atlantic Ocean, Atmospheric Chemistry and Physics, 10, 1555-1576, 10.5194/acp-10-1555-2010, 2010.

Whalley, L. K., Slater, E. J., Woodward-Massey, R., Ye, C., Lee, J. D., Squires, F., Hopkins, J. R., Dunmore, R. E., Shaw, M., Hamilton, J. F., Lewis, A. C., Mehra, A., Worrall, S. D., Bacak, A., Bannan, T. J., Coe, H., Percival, C. J., Ouyang, B., Jones, R. L., Crilley, L. R., Kramer, L. J., Bloss, W. J., Vu, T., Kotthaus, S., Grimmond, S., Sun, Y., Xu, W., Yue, S., Ren, L., Acton, W. J. F., Hewitt, C. N., Wang, X., Fu, P., and Heard, D. E.: Evaluating the sensitivity of radical chemistry and ozone formation to ambient VOCs and NOx in Beijing, Atmospheric Chemistry and Physics, 21, 2125-2147, 10.5194/acp-21-2125-2021, 2021.

Wu, R., Vereecken, L., Tsiligiannis, E., Kang, S., Albrecht, S. R., Hantschke, L., Zhao, D., Novelli, A., Fuchs, H., Tillmann, R., Hohaus, T., Carlsson, P. T. M., Shenolikar, J., Bernard, F., Crowley, J. N., Fry, J. L., Brownwood, B., Thornton, J. A., Brown, S. S., Kiendler-Scharr, A., Wahner, A., Hallquist, M., and Mentel, T. F.: Molecular composition and volatility of multi-generation products formed from isoprene oxidation by nitrate radical, Atmospheric Chemistry and Physics, 21, 10799-10824, 10.5194/acp-21-10799-2021, 2021.

Xiong, F., McAvey, K. M., Pratt, K. A., Groff, C. J., Hostetler, M. A., Lipton, M. A., Starn, T. K., Seeley, J. V., Bertman, S. B., Teng, A. P., Crounse, J. D., Nguyen, T. B., Wennberg, P. O., Misztal, P. K., Goldstein, A. H., Guenther, A. B., Koss, A. R., Olson, K. F., De Gouw, J. A., Baumann, K., Edgerton, E. S., Feiner, P. A., Zhang, L., Miller, D. O., Brune, W. H., and Shepson, P. B.: Observation of isoprene hydroxynitrates in the southeastern

590   United States and implications for the fate of NOx, Atmospheric Chemistry and Physics, 15, 11257-11272,
        10.5194/acp-15-11257-2015, 2015.
        Zare, A., Romer, P. S., Nguyen, T., Keutsch, F. N., Skog, K., and Cohen, R. C.: A comprehensive organic nitrate
        chemistry: insights into the lifetime of atmospheric organic nitrates, Atmospheric Chemistry and Physics, 18,
        15419-15436, 10.5194/acp-18-15419-2018, 2018.
595   Zaveri, R. A., Shilling, J. E., Fast, J. D., and Springston, S. R.: Efficient Nighttime Biogenic SOA Formation in a
        Polluted Residual Layer, Journal of Geophysical Research: Atmospheres, 10.1029/2019jd031583, 2020.
        Zhou, W., Zhao, J., Ouyang, B., Mehra, A., Xu, W., Wang, Y., Bannan, T. J., Worrall, S. D., Priestley, M., Bacak, A.,
        Chen, Q., Xie, C., Wang, Q., Wang, J., Du, W., Zhang, Y., Ge, X., Ye, P., Lee, J. D., Fu, P., Wang, Z., Worsnop, D.,
        Jones, R., Percival, C. J., Coe, H., and Sun, Y.: Production of N2O5 and ClNO2 in summer in urban Beijing, China,
600   Atmospheric Chemistry and Physics, 18, 11581-11597, 10.5194/acp-18-11581-2018, 2018.
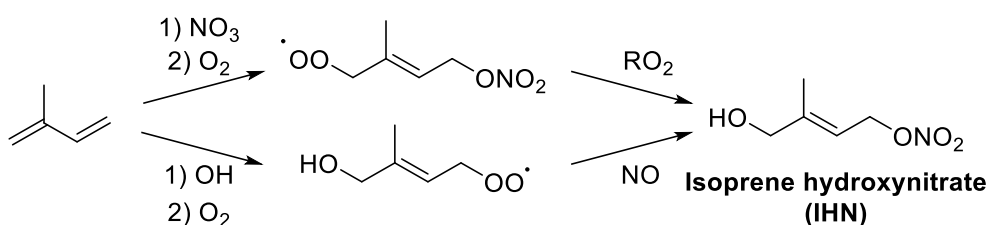
Figure 1. OH-initiated and NO₃-initiated formation of IHN. The formation of 1,4-IHN is shown here, other IHN isomers, as well as
605   **additional reaction products, will also be formed.**
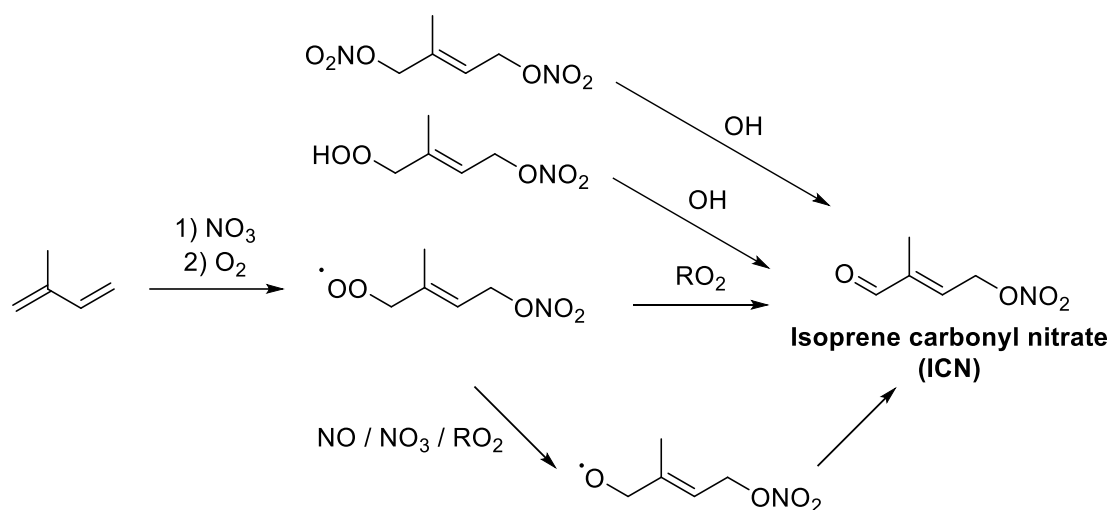
Figure 2. NO₃-initiated formation of ICN. The formation of 1,4-ICN is shown here, other ICN isomers, as well as additional
reaction products, will also be formed.
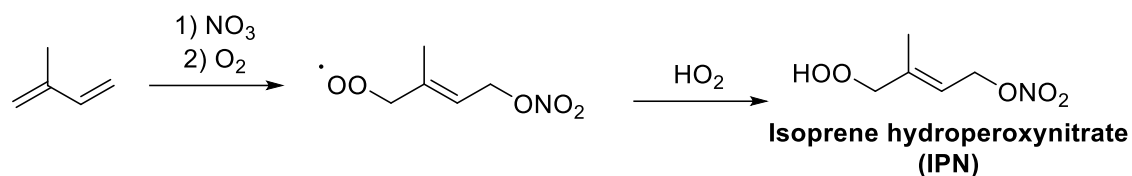
Figure 3. NO$_3$-initiated formation of IPN. The formation of 1,4-IPN is shown here, other IPN isomers, as well as additional reaction products, will also be formed.
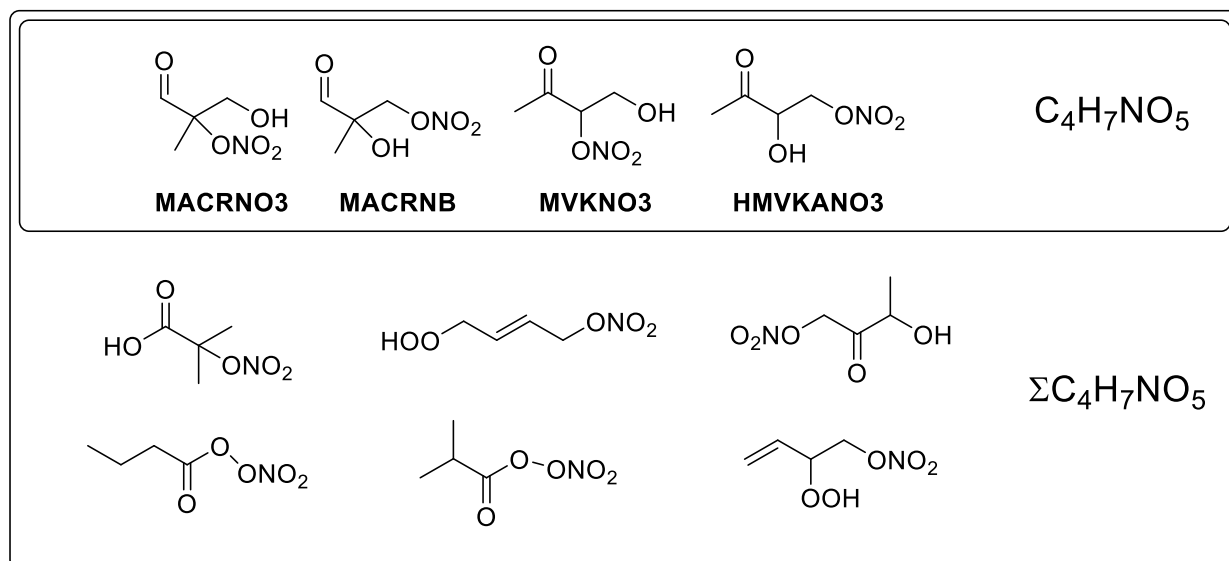
Figure 4. The four C$_4$H$_7$NO$_5$ species resulting from isoprene oxidation present in the MCM along with the additional isomeric compounds which complete the set of ΣC$_4$H$_7$NO$_5$
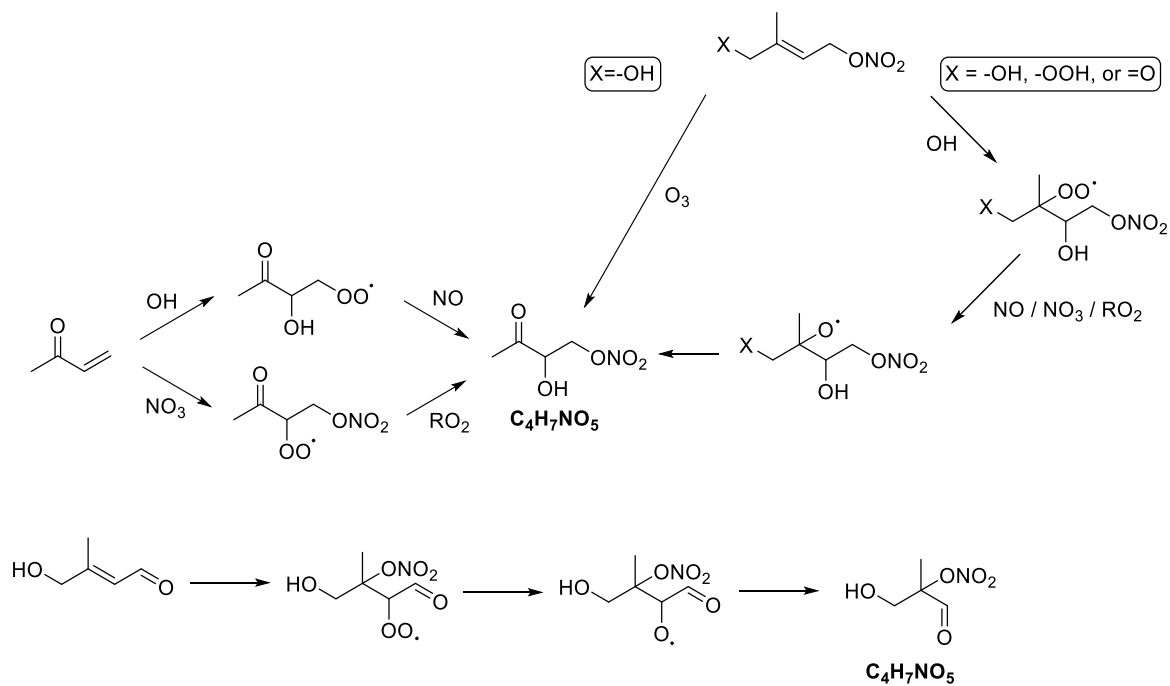
Figure 5. Formation of C₄H₇NO₅ compounds. Only two isomers are shown here, other formation routes for these and other isomers are also present. Additional reaction products will also be formed.

615
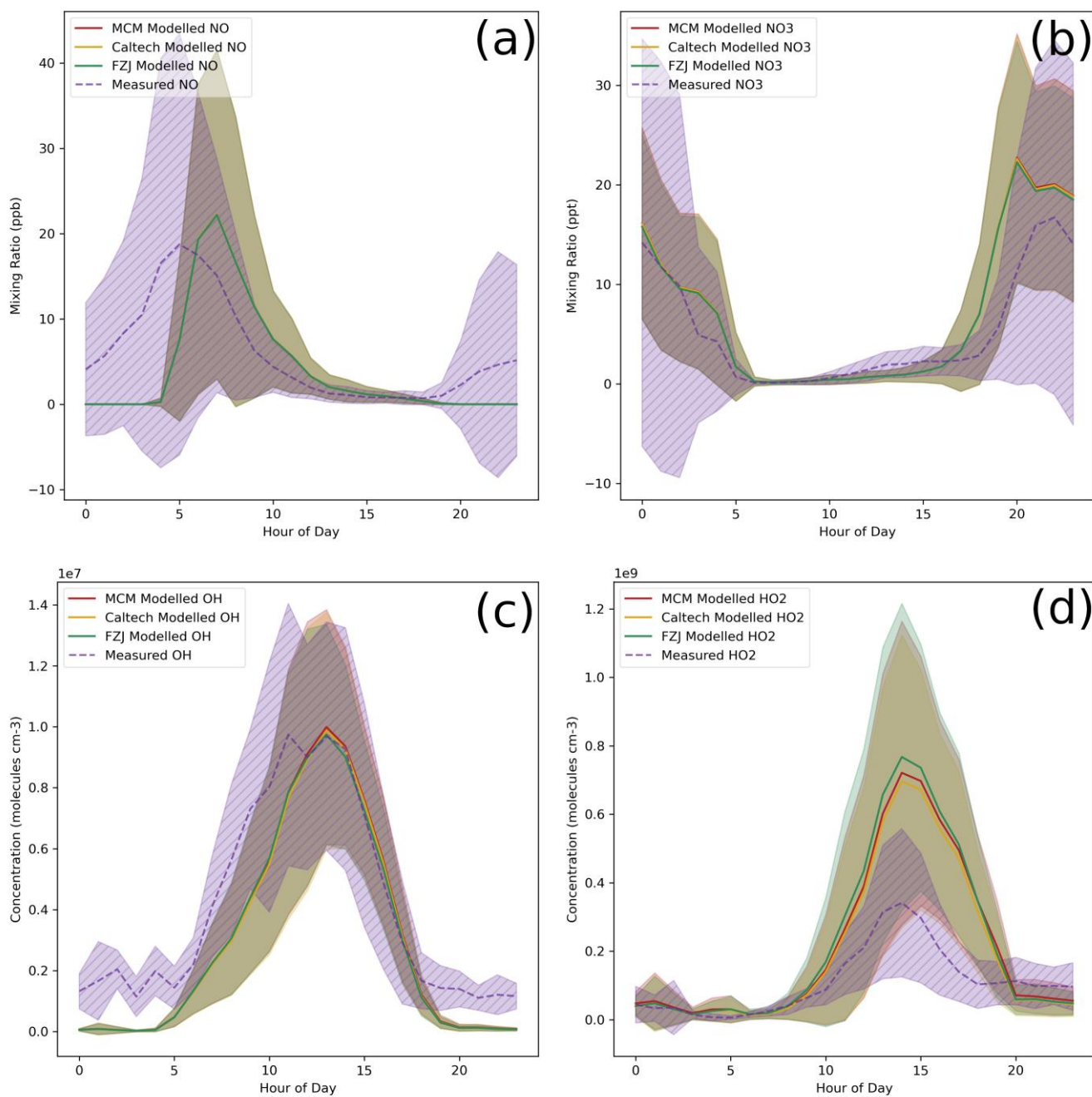
Figure 6. A selection measured values and model predictions of inorganic species left unconstrained in the models. Each line shows the mean value for each dataset, with the shaded area indicating one standard deviation above and below the mean.
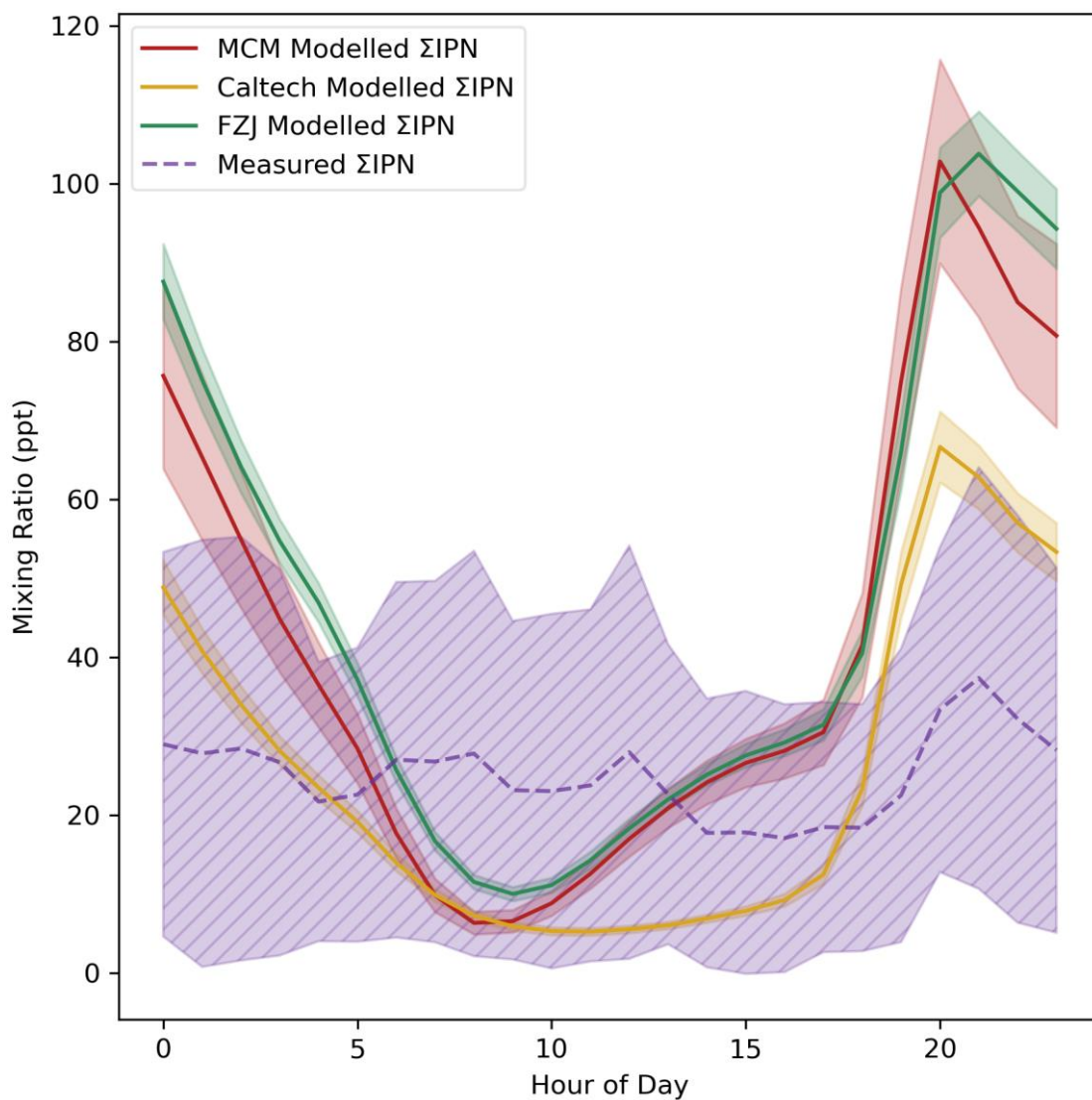
Figure 7. Measured and modelled ΣIPN (a). Each line shows the mean value for each dataset, with the shaded area indicating one standard deviation above and below the mean.
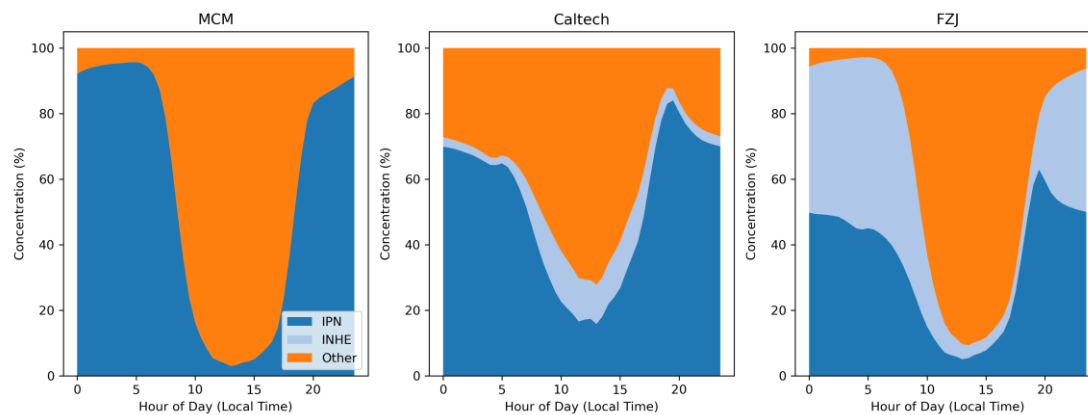
Figure 8. Isomer composition of the modelled ΣIPN as a percentage of total ΣIPN. "Other" comprises of ISOP1N253OH4OH, C530NO3, PPEN, C524NO3, C51NO3, and C5PAN4.
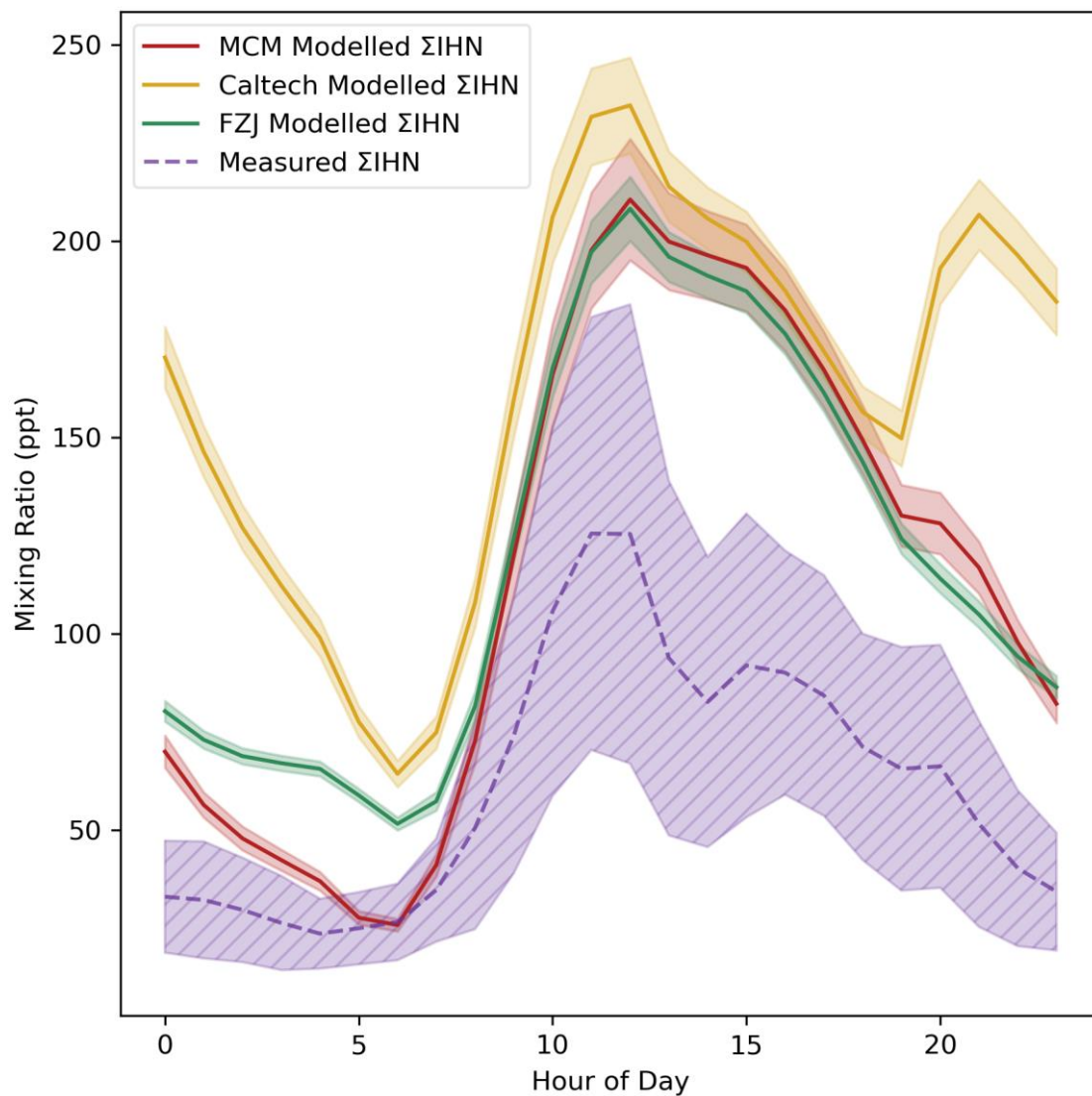
Figure 9. Measured and modelled ΣIHN. Each line shows the mean value for each dataset, with the shaded area indicating one standard deviation above and below the mean.
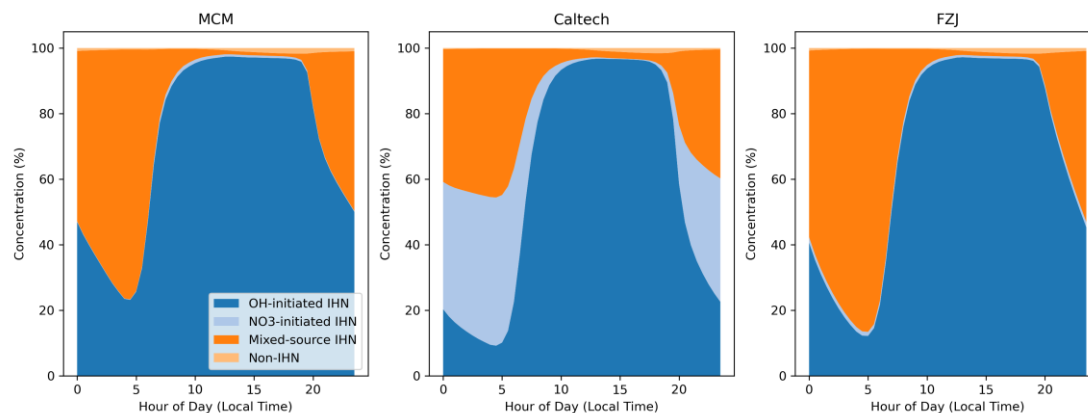
630

Figure 10. Isomer composition of the modelled ΣIHN. OH-initiated IHN are those primarily formed by OH chemistry, the 1,2-IHN and 4,3-IHN. NO3-initiated IHN are those primarily formed by NO3 chemistry, the 2,1-IHN and 3,4-IHN. Mixed-source IHN is formed in large amounts by both routes, the E/Z-1,4-IHN and E/Z-4,1-IHN.
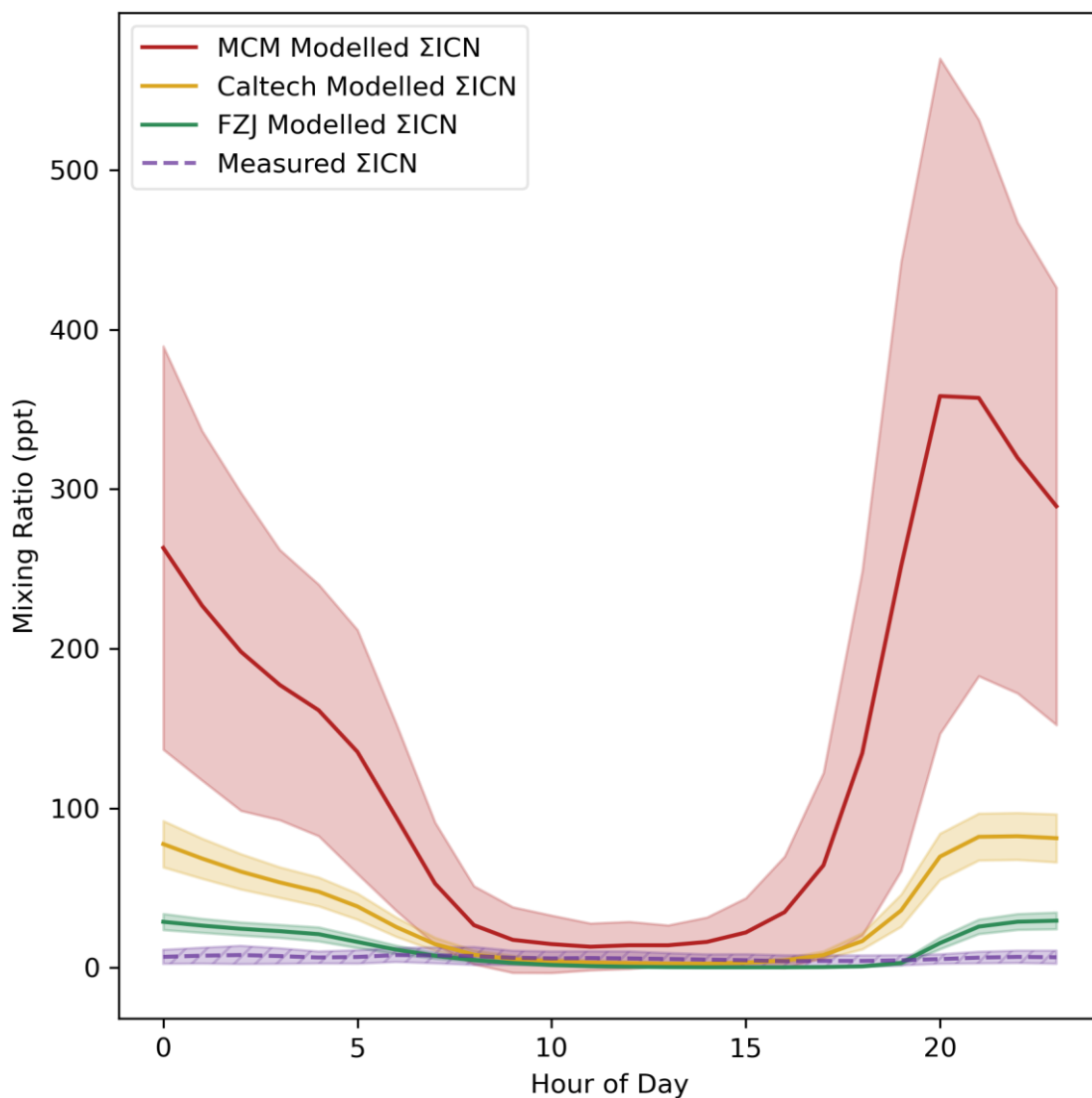
Figure 11. Measured and modelled ΣICN. Each line shows the mean value for each dataset, with the shaded area indicating one standard deviation above and below the mean.
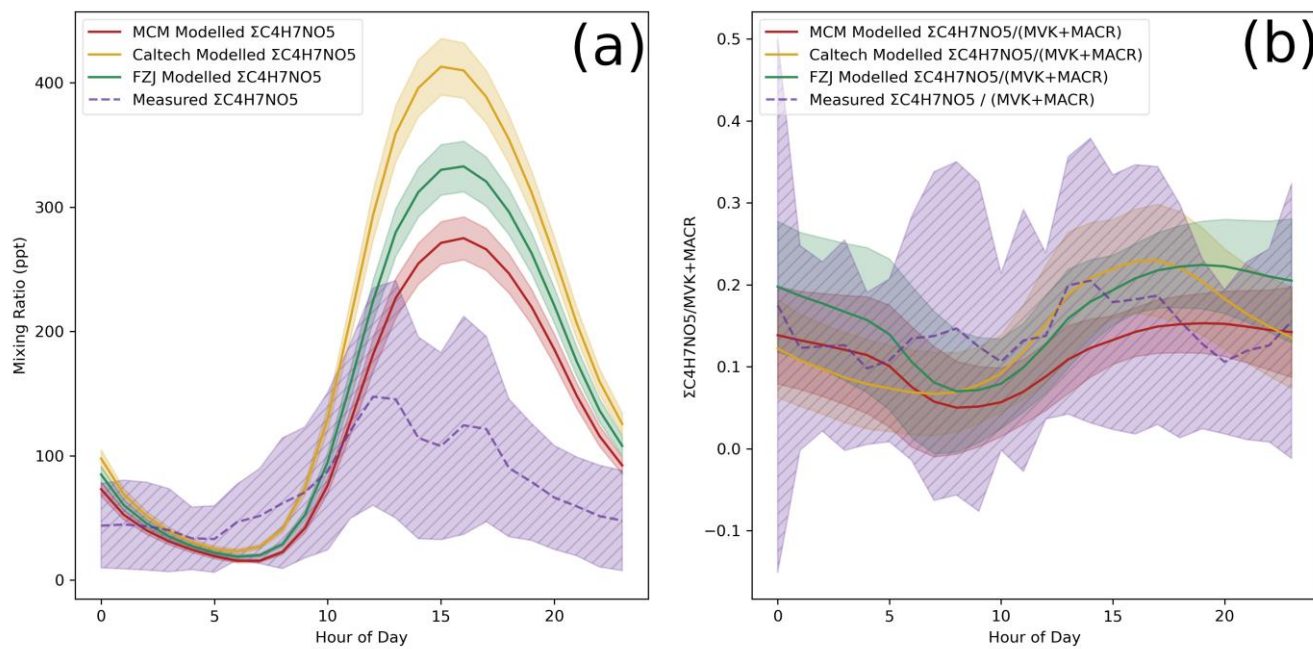
Figure 12. Measured and modelled (a) $\Sigma C_4H_7NO_5$ and (b) $\Sigma C_4H_7NO_5$/(MVK+MACR). Each line shows the mean value for each dataset, with the shaded area indicating one standard deviation above and below the mean.